Introduction

A

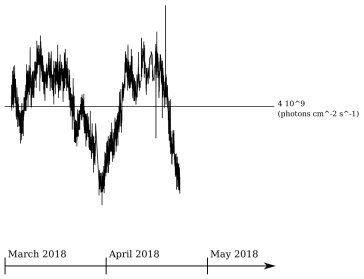

B

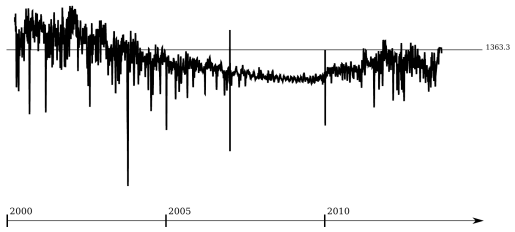

Figure 1 *(A) Extracts form satellite data records of photon flux deposited in Univ. of South Carolina site, radiation of Sun in 2018; (B) Radiation of Sun from 2000 to 2013 recorded by "ACRIM3" satellite.*

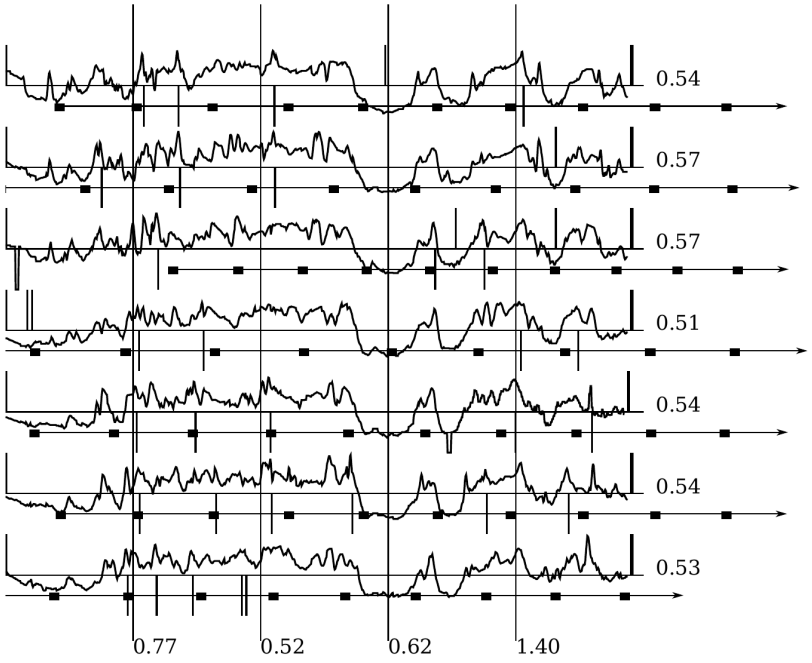

Figure 2 *Snapshot from video record of sun flaming 15.06.2002, deposited by Swedish physicists. Digits in column - Higuchi fractal dimension for spatial axis, digits in row - approximation of fractal dimension for time axis.*

Methods

Fitting of log-periodicity

A

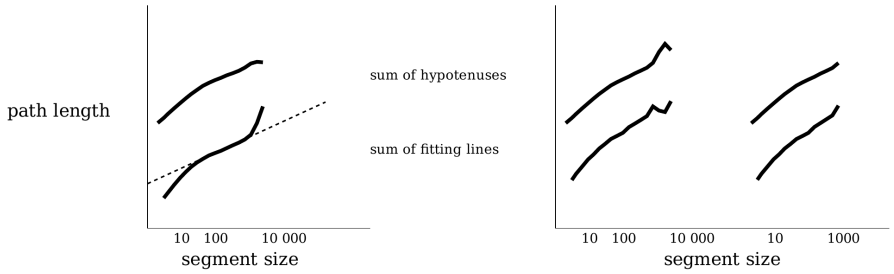

B

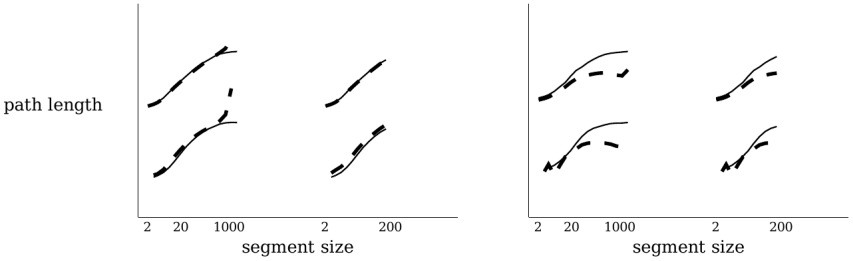

Figure 3 *Illustrations of attempts to guess a presence of the log-periodic dependency (A) Uniform distribution - chart in fig. 1A (B) Periodic bursts - chart in fig 1B, two talils in separate.*

Table 1 *Supplement to figure 3 - results of fitting of log-periodicity in log-log distributions*

	usc_18		acrim3-1		acrim3-2	
	method 1	method 2				
plain:						
dimension	0.577973	0.579382	0.691307	0.747027	0.598869	0.645797
correlation	-0.983925	-0.969044	-0.984111	-0.97212	-0.974277	-0.959029
fit in full:						
direction	decc.	decc.	accel.	accel.	accel.	accel.
critical time	-711	-141	+318	+474	+6	+8
dimension	0.686096	0.880372	0.858975	1.07331	0.881265	0.788433
correlation	-0.992609	-0.996231	-0.998645	-0.998409	-0.998075	-0.979409
fit in part:						
direction	accel.	decc.	decc.	accel.	accel.	accel.
critical time	+2	-141	-474	+2	+63	+3
dimension	0.677549	0.949008	0.822429	0.949565	0.599305	0.974975
correlation	-0.992127	0.996914	-0.996929	-0.99992	-0.995057	-0.999909

Input measurements

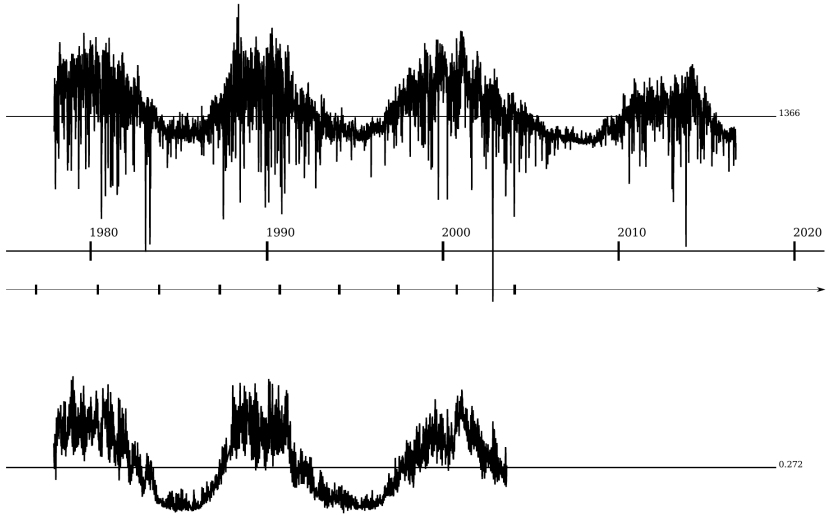

Figure 4 *Radiation of Sun in period from November 1978 to September 2017; in bottom - radiation at MgII frequency.*

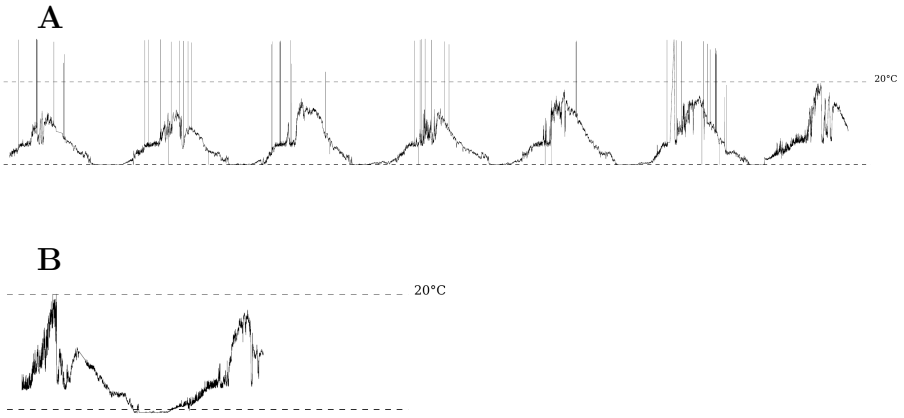

Figure 5 *Temperature of water in Baikal (A) series from May 2010 to October 2016; (B) series from May 2017 to September 2018.*

Results

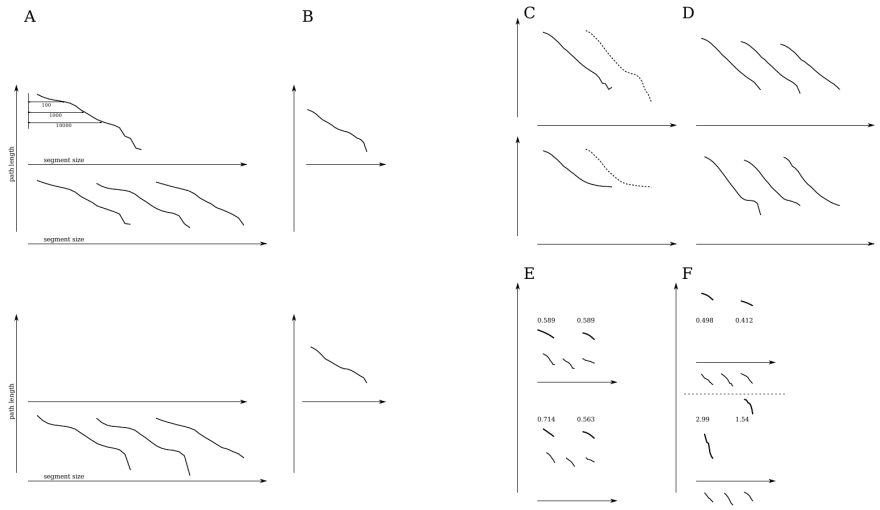

Figure 6 *Log-log dependencies, for the two types of method. A,B: temperature in Baikal, A - 2010-2016, B - 2017-2018 period, C,D: solar activity, 1978-2017, E,F - fragments of auxiliary records on solar irradiation*

In A,D, three separate lines are the distributions for beginning, middle and ending parts of a period. Dashed lines in C, for a comparison - path lengths are estimated by the modified approach, suitable to fitting of log-perodicity. In E,F, - time series are of 15.06.2002 as in fig.2, and of 01.04.2018 as in fig1B, at average and in a few randomly choosed parts. Appropriate fragments from the long-time series, shown in fig 4 and here in C,D, are added for a comparison; numerical labels are estimated least-square slopes of regression lines.

That is, the measure of fractal dimension is consistent for mulitiple data sources. And, the interval $s < 10$ is most sensitive (in fig 6A) to a change of time period.

Table 2

	method 1 dimension	correlation	*method 2* dimension	correlation
Solar activity, *total*, 1-10 t.p.				
period 1, at a whole	0.611359	-0.98176	-0.98176	-0.992606
period 1, split to 10 parts	0.620717 ± 0.0686381		0.633088 ± 0.117143	
period 2, at a whole	0.582742	-0.980571	0.56841	-0.987462
period 2, split to 10 parts	0.577533 ± 0.0646417		0.57153 ± 0.0621609	
period 3, at a whole	0.529598	-0.98341	0.940431	-0.961894
period 3, split to 10 parts	0.543816 ± 0.117594		0.674605 ± 0.273296	
MnII intensity,				
1...10 t.p., at a whole	0.349931	-0.975307	0.439804	-0.942881
1...10 t.p, split to 10 parts	0.345247 ± 0.102797		0.35548 ± 0.195736	
1...max t.p., at a whole	0.531589	-0.960948	0.560595	-0.930574
1...max t.p, split to 10 parts	0.679449 ± 0.0622246		0.774685 ± 0.109925	
Temperature in Baikal				
long series; 1...10 t.p.				
period 1, at a whole	0.570939	-0.992162	0.812175	-0.995154
period 1, split to 10 parts	0.613501 ± 0.126926		0.868055 ± 0.177196	
period 2, at a whole	0.532256	-0.991045	0.739015	-0.994156
period 2, split to 10 parts	0.633994 ± 0.217527		0.876311 ± 0.29755	
period 3, at a whole	0.303322	-0.99865	0.385959	-0.995293
period 3, split to 10 parts	0.364181 ± 0.227035		0.467551 ± 0.320929	
short series				
1...80 t.p., at a whole	0.606348	-0.995202	0.662082	-0.988346
1...80 t.p., split to 10 parts	0.564113 ± 0.164664		0.628443 ± 0.215225	
40...80 t.p., at a whole	0.508056	-0.981986	0.507846	-0.99867
40...80 t.p, split to 10 parts	0.425593 ± 0.28323		0.444415 ± 0.282211	

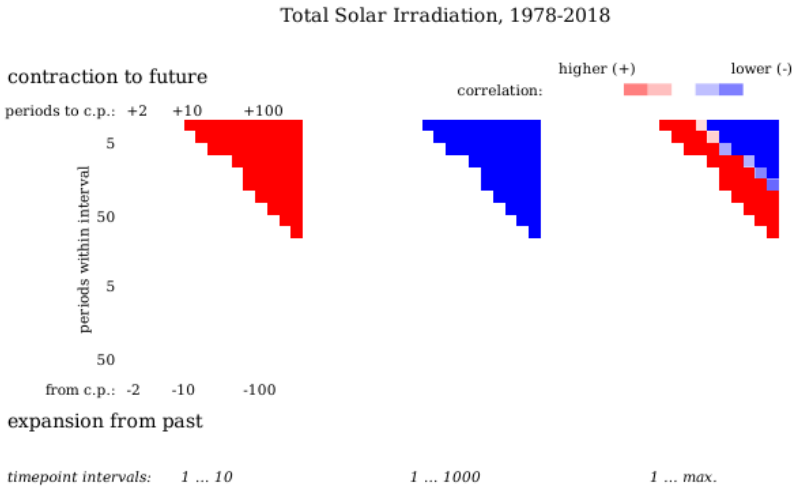

Figure 7 *Fitting of log-periodicity. Explanation.*

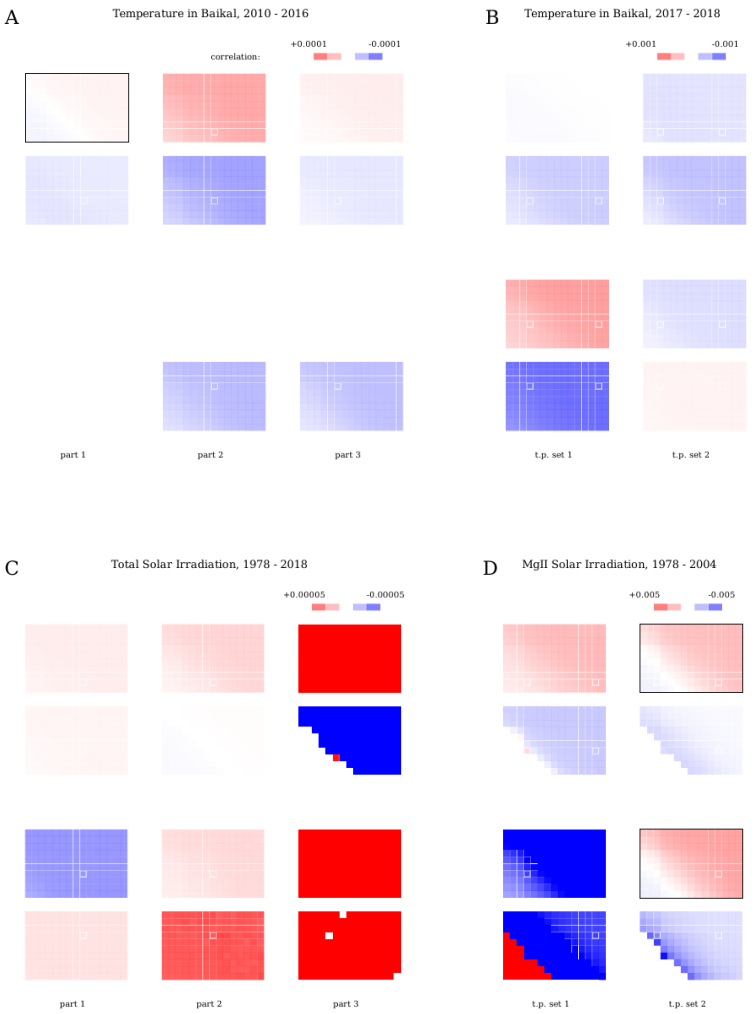

Figure 8 *Fitting of log-periodicity. Accordingly to table 2.*

That is, for data in fig 8A, a trend to contraction to up-going crisis is observed in the first row. The same trend can be seen in fig 8D for solar activity.

Conclusions

The crisis on Baikal which began at around 2014 was possible to detect by slightly unusual variations of water temperature in two to four years before (fig 9 A).

If a covid-19 is not an ordinary virus pandemy, to what extent is this extraaordiunarity expanded? The exclusive search gave similarity of "projection" to a model of log-periodic acceleration between variations of temperature in Baikal before crisis, and variations of intensity of solar irradiation in past 30 years (fig. 9B), this can point out to expectations of universe-scale crisis in a near future.

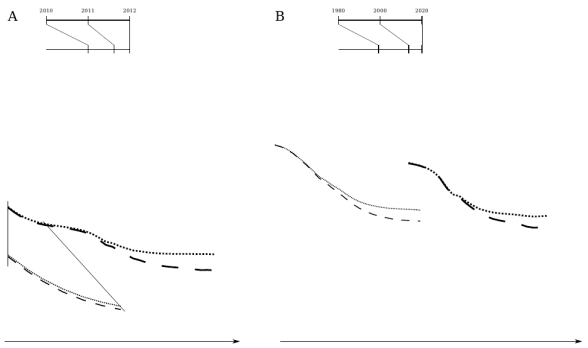

Figure 9 *Concluding drawing.*

References

1. Nottale, L., Scale relativity and fractal space-time: theory and applications, *arxiv.org*, 2008
2. Feranchuk, S., Belkova, N., et al. *Limnology and Freshwater Biology*, 2018,

Appendix A

```
 cat usc_18.txt | awk -v i=0 -v b1=2458119.5 -v b13=7 '{ if ( i == 100 && substr(
$13, 1, 1 ) != "0" ) { s = s "," 10 * ( $1 - b1 ) "," 500 * (substr($13,1,7)
- b13 ); i = 0; }; i = i+1; } END { print substr( s, 2 ) }' | ./fractal_dimension
-d_xy
```